Appl Microbiol Biotechnol (2011) 89:1423–1433
DOI 10.1007/s00253-011-3101-1

Sustained release of PI3K inhibitor from PHA nanoparticles and in vitro growth inhibition of cancer cell lines

Xiao-Yun Lu · Elisa Ciraolo · Rachele Stefenia · Guo-Qiang Chen · Yali Zhang · Emilio Hirsch

Received: 15 October 2010 / Revised: 20 December 2010 / Accepted: 21 December 2010 / Published online: 1 February 2011

Abstract The phosphoinositide-3-kinases (PI3Ks) are a conserved family of lipid kinases that phosphorylate the 3-hydroxyl group of phosphatidylinositols in response to extracellular stimuli. PI3K pathway is enrolled in different kinds of human cancer and plays a prominent role in cancer cell growth and survival. Several PI3K inhibitors have been recently identified but some PI3K inhibitors with high potency in vitro do not show satisfactory effects in animal cancer models because of the poor pharmaceutical properties in vivo such as poor solubility, instability, and fast plasma clearance rate. In this study, we developed a sustained release system of PI3K inhibitor (TGX221) based on polyhydroxyalkanoate nanoparticles (NP) and used it to block proliferation of cancer cell lines. TGX221 was gradually released from PHA-based NP and growth of cancer cell lines was significantly slower in NP-TGX221-treated cells than in either negative controls or in cells receiving free TGX221. Since poor bioavailability and limited in vivo half-life are common features of hydrophobic PI3K inhibitors, our results open the way to similar formulation of other PI3K blockers and to new strategies in cancer treatment.

Keywords Polyhydroxyalkanoate · PI3K inhibitor · TGX221 · Nanoparticle · Drug delivery

X.-Y. Lu · Y. Zhang
Department of Biological Science and Bioengineering,
Key Laboratory of Biomedical Information Engineering
of Ministry of Education, School of Life Science and Technology,
Xi'an Jiaotong University,
Xi'an 710049 Shaanxi, People's Republic of China
e-mail: emilio.hirsch@unito.it

X.-Y. Lu
e-mail: luxy05@mail.xjtu.edu.cn

X.-Y. Lu · E. Ciraolo · R. Stefenia · E. Hirsch
Molecular Biotechnology Center, Università di Torino,
Via Nizza 52,
10126 Turin, Italy

G.-Q. Chen
Department of Biological Sciences and Biotechnology,
Tsinghua University,
Beijing 100084, People's Republic of China

Present Address:
X.-Y. Lu
School of Life Science and Technology, Xi'an Jiaotong University,
No. 28 West Xianning Road,
Xi'an 710049 Shaanxi, People's Republic of China

Introduction

The application of nanotechnology has significantly affected the development of drug delivery systems as it provides significant advantages compared to conventional strategies (Shi et al. 2010). For example, it could improve the therapeutic activity of drugs by enhancing their bioavailability and their effectual concentration, improving solubility of hydrophobic drugs and prolonging half-life. It could also reduce the toxic side effects by releasing drugs in a sustained or stimuli-triggered manner. In addition, nanoparticles could be passively accumulated in specific tissues such as tumor or inflammatory tissues through the enhanced permeability and retention effect (Langer 1998). Many different materials including liposome, polymers, and some self-assembled macromolecules have been developed as drug delivery carriers (Mundargi et al. 2008). Among these, biodegradable polymers are of interest because of their flexibility and biocompatibility properties.

Polyhydroxyalkanoates (PHA) are aliphatic biopolyesters which are synthesized by a wide range of bacteria as the energy- and carbon-storage materials. Based on their different 3-hydroxyalkanoate (3HA) monomers structure composition and contents, PHAs demonstrate various physicochemical properties and kinetics of biodegradation (Steinbuchel 2001; Liu and Chen 2008). Because of their good biocompatibility and biodegradability, PHAs have been studied for implant biomedical and controlled drug-release applications (Sun et al. 2007; Xiao et al. 2007; Wu et al. 2009; Xiong et al. 2010). In the past, some success was reported with the use of polyhydroxybutyrate (PHB), poly(3-hydroxybutyrate-*co*-3-hydroxyvalerate) (PHBV), and poly(3-hydroxybutyrate-*co*-3-hydroxyhexanoate) (PHBHHx) as controlled drug release matrices (Koosha et al. 1989; Saad et al. 1996a, b; Gursel et al. 2001; Wang et al. 2003; Rossi et al. 2004; Lu et al. 2010; Xiong et al. 2010). They were more efficient in encapsulating the hydrophobic compounds due to their aliphatic polymer properties and thus would be beneficial especially for hydrophobic drugs such as phosphoinositide-3-kinases (PI3Ks) inhibitors.

PI3Ks are a conserved family of lipid kinases that phosphorylate the 3-hydroxyl group of phosphatidylinositols (PtdIns) in response to extracellular stimuli. PI3Ks have important regulatory roles in multiple cellular processes, including cell survival, proliferation, differentiation, migration, and metabolism. PI3Ks could be divided into four classes (Leevers et al. 1999). The best characterized members of PI3K family are the class I PI3Ks. Mammals possess four class I PI3Ks usually termed PI3Kα, β, γ, and δ. While PI3Kα and β are ubiquitously expressed, the expression of PI3Kγ and δ is largely restricted to the immune system (Vanhaesebroeck et al. 1997). Recent progress in genomic studies and cancer biology have indicated that components of the PI3K pathway play a prominent role in cell growth and survival and are critically involved in cancer. This pathway is frequently found activated in human cancer as a result of mutations or amplification of the PI3K enzymes or alterations involving their upstream and downstream signaling players, such as receptor tyrosine kinases (RTKs), the serine/threonine protein kinase Akt/PKB, or phosphatase and tensin homolog (PTEN) (Bader et al. 2005; Thomas et al. 2007; Chin et al. 2008; Keniry and Parsons 2008; Parsons et al. 2008). Therefore, inhibition of PI3K appears to represent a promising strategy in cancer therapy. Several PI3K inhibitors have been identified and some are currently under clinical development (Liu et al. 2009). Nonetheless, several PI3K inhibitors with high potency in vitro did not show sufficient efficacy in vivo in animal models of cancer. This is often due to poor pharmaceutical properties in vivo such as limited solubility, insufficient stability, and fast plasma clearance rate. Such drawbacks frequently represent the key obstacles to further clinical development of PI3K inhibitors. In contrast, using nanoscale delivery vehicles, pharmacological properties of such weak drug candidates could be significantly improved. In this study, we developed a sustained release system based on PHAs nanoparticle (NP) loaded with TGX221, a PI3K inhibitor, and used it to control growth of different cancer cell lines.

TGX221 is described as a PI3K p110β selective inhibitor which is an ATP competitive kinase inhibitor. The IC_{50} values for TGX-221 against two main class I PI3K catalytic isoforms p110α and p110β are 5 μM and 5–9 nM, respectively (Jackson et al. 2005; Chaussade et al. 2007). It could inhibit the growth of PTEN-deficient cancer cell lines (Wee et al. 2008) and ErbB2-driven tumors (Ciraolo et al. 2008). It has been widely used as one of the very few p110β-selective inhibitors but failed in different preclinical trials because of poor solubility and very short circulating half-life. In this study, we entrapped TGX221 into PHA nanoparticles and investigated its release and cytostatic activity in cell-based assays.

Materials and methods

Materials

Poly(3-hydroxybutyrate) with a weight-average molecular weight (Mw) of 6×10^5, poly(3-hydroxybutyrate-*co*-12 mol % 3-hydroxyhexanoate) (PHBHHx) (Mw=4×10^5) were donated by Lab of Microbiology, Department of Biological Science and Biotechnology, Tsinghua University (Beijing, People's Republic of China). Poly(3-hydroxybutyrate-*co*-5 mol% 3-hydroxyhexanoate) (PHBV) (Mw=4×10^5) was purchased from Tianan Biomaterials Co. Ltd. (Ningbo, People's Republic of China). Poly(vinyl alcohol) (PVA) (Mw=2.2×10^4, 88% hydrolyzed) and poly(DL-lactide-*co*-glycolide) (PLGA 75:25) (Mw=1×10^5) were purchased from Sigma-Aldrich (USA). TGX221 was kindly donated by Prof. Galli Ubaldina, University of Novara (Novara, Italy).

Preparation of TGX221-loaded nanoparticles

The TGX221-loaded nanoparticles were fabricated by a modified emulsification/solvent diffusion method (Perez et al. 2001; Xiong et al. 2010). In this study, four types of hydrophobic polymer nanoparticles (PHB, PHBV, PHBHHx, and PLGA) were prepared *via* ultrasonication. Briefly, 50 mg of polymers and 5 mg of TGX221 were added into 1 ml chloroform, and the mixture was stirred to ensure that all materials were dissolved. Twenty milliliters of 1% PVA (w/v) was sonicated for 1 min and was slowly added with 1 ml of organic solution. The double emulsion

was then deal with sonication using a probe sonicator (Sonics & Materials, Newtown, CT, USA) for 5 min and the mixed solution was moderately stirred with a magnetic mixer for 6 h to solidify the nanodroplets. Chloroform was removed by volatilization at room temperature. The nanoparticles were collected by centrifugation at 38,000 rpm for 60 min, followed by washing twice with deionized water.

Characterization of nanoparticles

The particle size and zeta potential were measured by a laser light scattering machine (Zetasizer Nano ZS, Malvern, UK). The samples were diluted into proper concentration with deionized water and examined to determine the average particle diameters and zeta potential.

Efficiency and drug-loading content measurement

The drug entrapment efficiency refers to the amount of TGX221 loaded into the nanoparticles as compared with the total amount used in the loading process. The drug-loading content (DLC) was defined as the TGX221 entrapped as compared with the total amount of drug-loaded nanoparticles. The TGX221 entrapment efficiency and drug loading content were calculated according to Eqs. (1) and (2).

$$\text{Entrapment efficiency}\,(\%) = (M_t/M_i) \times 100\% \quad (1)$$

$$\text{Drug} - \text{loading content}\,(\%) = (M_t/M_p) \times 100\% \quad (2)$$

Where M_p represented for the mass of NPs, M_i is the mass of TGX221 fed initially, and M_t represented for the total amount of TGX221 in PHAs nanoparticles (Li et al. 2008). The amount of TGX221 was analyzed by high performance liquid chromatography (HPLC) with an Xterra C18 column (2.5 μm, 2.0×15 mm; Waters Corporation, MA, USA). Briefly, 2 mg of TGX221-loaded nanoparticles were dissolved in 10 ml acetonitrile at 60°C and followed by being stored at 4°C for 4 h to precipitate PHA. The supernatant was used to perform the HPLC analysis after filtrated with 0.2 μm filter.

The absorbed TGX221 onto the surface of PHB nanoparticles were also analyzed as follows: 10 mg of PHB nanoparticle suspended in 1 ml of PBS were incubated with 1 mg of TGX221 dissolved in 5 ml ethanol at 4°C overnight. Nanoparticles were collected and resuspended in 1 ml PBS. Fifty microliters of resuspended nanoparticles was dissolved in 450 μl acetonitrile at room temperature and then stored at −20 °C to precipitate polymer. The supernatant was analyzed by HPLC after filtration.

In vitro drug release study

In vitro release studies of TGX221 from PHB, PHBV, PHBHHx, and PLGA nanopartilces were performed by the dialysis bag method (Li et al. 2008). Briefly, 10 mg NPs/MPs powder was suspended in 5 ml of phosphate buffered saline (PBS) and placed in a dialysis membrane bag with a molecular weight cutoff of 6000 g/mol. The bag was tied and immersed into 100 ml of a phosphate buffer solution (pH 7.4). The entire system was kept at 37 °C with continuous stirring. Then 0.5 ml of the aqueous solution was taken out of the release medium at predetermined time intervals, replaced by fresh PBS buffer. The aqueous solution was then measured by HPLC as described above and the release amount of TGX221 was determined by a calibration curve. The reported values are the mean values for three replicate samples. The total amount of TGX221 (M_t) in 10 mg nanoparticles was determined by the method mentioned in the previous section. The release percent was calculated according to Eq. (3)

$$\text{Released percentage}\,(\%) = (M_r \times 100/0.5 \times M_t) \times 100\% \quad (3)$$

Where M_r represented the amount of TGX221 in 0.5 ml of the aqueous sample solution and M_t represented the total amount of TGX221 in nanoparticles.

Cell culture and proliferation assay

All cell lines used were the preservation of Molecular Biotechnology Center, Universita di Torino, Turin, Italy. NIH/3T3 fibroblast cell line and BT-474 human breast cancer cell line were cultivated in Dulbecco's modified essential medium containing GlutaMAX and 4.5 g/l glucose (Invitrogen, USA) supplemented with 10% fetal bovine serum and 1% penicillin–streptomycin at 37 °C in humidified environment of 5% CO_2. PC3 human prostate cancer cell line and HCT-116 large intestine colon carcinoma cell line were maintained in RPMI 1640 and McCoy's 5A medium (Invitrogen), respectively, supplemented with 10% fetal bovine serum. The medium was replenished every other day and the cells were subcultured after reached confluence.

For measurement of proliferation, cells were seeded in triplicate at 2×10^3 cells/well in 96-well culture plates and incubated overnight to allow cell attachment. The cells were incubated with the TGX221-loaded PHA nanoparticles, empty PHA nanoparticles, or free TGX221 for 24, 48, and 72 h. At designated time intervals, cells were quantified by a crystal violet staining-based colorimetric assay (Kueng et al. 1989). Briefly, cells were fixed by addition of 100 μl of 2.5% glutaraldehyde solution and

incubated at room temperature for 30 min. Plates were washed three times by submersion in PBS solution. Plates were air-dried and stained by addition of 100 μl of 0.1% solution of crystal violet dissolved in deionized water and incubated for 20 min at room temperature, excess dye was removed by extensive washing with deionized water, and plates were air-dried prior to bound dye solubilization in 100 μ1 of 10% acetic acid. The optical density of dye extracts was measured directly in plates using a microplate reader (Bio-Rad Laboratories, Inc., UK) at 570 nm.

PI3K inhibition assay and western blot analysis

NIH 3T3 cells were seeded in 96-well plates at 10,000 cells/well and incubated at 37 °C with 5% CO_2 in a humidified incubator. Before the inhibition assay, cells were first starved in serum-free DMEM for 16 h and then treated with TGX221 or drug-loaded PHB nanoparticle at 0.2, 2, and 20 μM, respectively, for 2 h. Cells were then stimulated with LPA (10 μM) and insulin (1 μM) for 5 min to test the inhibition effect of p110β and p110α, respectively. Cells were lysated by adding 1× Laemmli SDS–PAGE buffer (Tris–HCl 63 mM, glycerol 10%, SDS 2%, bromophenol blue 0.0025%, pH 6.8) and extracted proteins were then loaded into 10% SDS–PAGE gels. After electrophoresis, proteins were transferred on to PVDF membranes, which were then blocked for 1 h at room temperature with 5% bovine serum albumin in TBS buffer. PVDF membrane was incubated overnight with an anti-phospho-Akt (Ser 473) antibody purchased from Cell Signaling Biotechnology (#9271) and anti-β-actin antibody from Santa Cruz Biotechnology (Santa Cruz, CA, USA). The PVDF membrane was subsequently hybridized with secondary HRP conjugated anti-rabbit IgGs (Sigma Aldrich #A6154) and the amount of phosphorylated Akt was detected by incubating with a chemiluminescence solution (ECL) purchase from Millipore (#WBKLS0050).

Statistical analysis

All results were expressed as mean±standard deviation of experiment performed in triplicates. Statistical differences were evaluated using a one-way analysis of variance (ANOVA) with Student's *t* test. Differences were considered to be statistically significant at a level of $P < 0.05$.

Results

Preparation and characterization of nanoparticles

Four kinds of nanoparticles (PLGA, PHB, PHBV, and PHBHHx) and three kinds of TGX221-loaded nanoparticles (PLGA, PHB, and PHBHHx) were prepared by emulsification–solvent evaporation technique. The sizes, polydispersities, and surface charges of the nanoparticles are listed in Table 1. Figure 1 shows the size distribution of nanoparticles and TGX221-loaded nanoparticles with various diameters which were prepared from PLGA and PHAs, respectively. The diameter of nanoparticles mainly depended on the shearing force during the preparation and small nanoparticles could be achieved by intense stirring. The sizes of nanoparticles ranged from 100 to 300 nm after 3–6 h stirring with relative low polydispersity index (PDI).

All nanoparticle preparations exhibited negative zeta potential values which ranged from −10 to −27 mV. Compared with PLGA nanoparticles, PHA nanoparticles showed more negative surface charges (especially the PHBHHx nanoparticle). This impacted on stability of the nanoparticle suspension because the negative zeta potential of the nanoparticles is directly proportional to the dispersion stability of the nanoparticles in the medium (Jeong et al. 2009). The TGX221-loaded nanoparticles showed relative low zeta potential values, possibly due to the absorption of the hydrophobic drug on the surface of nanoparticles that reduced the ionization of the stationary layer of fluid attached to the dispersed nanoparticle. The PHA nanoparticles formed an incipient stable colloidal suspension in aqueous medium which could be stored for at least 1 month without aggregation.

In terms of entrapment efficiency of TGX221, PHA nanoparticles showed the highest ranking. While PLGA nanoparticles showed only 65% efficiency, PHA nanoparticles that made from PHBHHx reached a peak of 97% efficiency. The drug-loading content of TGX221 in PHA nanoparticles was around 8.5–8.8%. To further assess the entrapment efficiency, the amount of TGX221 absorbed onto the surface of PHB nanoparticles was analyzed. Results showed that about 930 μg of TGX221 can be detected in 10 mg of TGX221-loaded nano-

Table 1 The sizes, polydispersities, and zeta potential of the free and TGX221-loaded nanoparticles

NP/NP-TGX	Size (nm)	PDI	Zeta potential (mV)	Entrapment efficiency (%)
PLGA	211±5	0.074±0.02	−13.4±3	–
PHB	220±3	0.107±0.03	−18.2±2	–
PHBV	221±4	0.103±0.03	−15.5±1	–
PHBHHx	195±2	0.053±0.01	−24.8±1	–
PLGA-TGX	222±6	0.069±0.02	−9.3±1	65±2
PHB-TGX	223±4	0.099±0.04	−9.9±2	93±1
PHBHHx-TGX	206±4	0.073±0.03	−14.9±1	97±2

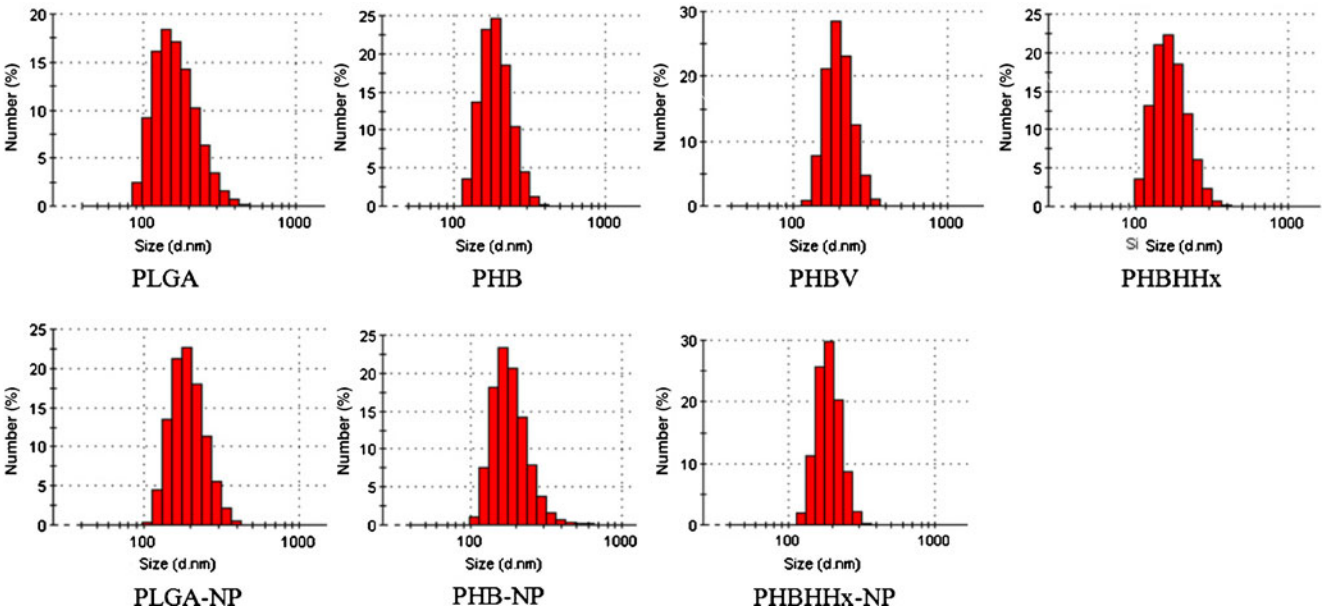

Fig. 1 The size distribution of free and TGX221-loaded nanoparticles determined by dynamic light scattering

particles, while only 60 μg of TGX221 can be absorbed onto the surface of 10 mg PHB nanoparticles. This indicates that only a small part of TGX221 was absorbed on the surface of PHB nanoparticle and that most of the drug was incorporated within the particle. Because of the high potency of TGX221 against p110β isoform, this drug-loading efficiency was considered sufficient for subsequent experiments.

In vitro release of TGX221 from nanoparticles

Three kinds of TGX221-loaded nanoparticles were prepared based on PLGA, PHB, and PHBHHx, respectively. Figure 2 shows the in vitro release profiles of TGX221-loaded nanoparticles in PBS at 37 °C. All different nanoparticles showed similar profiles of an initial burst release followed by a sustained discharge stage. Interestingly, at the initial phase, the release of TGX221 from PHBHHx nanoparticles was faster than from either PHB or PLGA nanoparticles. Indeed, in PHBHHx nanoparticles, about 76% of the drug was released within the first 32 h. Such behavior might be due to the relative low level of crystallized PHBHHx material, thus allowing TGX221 to diffuse from the loose particle core. On the contrary, the initial release of TGX221 from PHB and PLGA nanoparticles was slower, showing around 42% and 54% of drug release within the first 32 h, respectively. Although the release of TGX221 from PLGA nanoparticles during the initial stage was slower than that from PHBHHx nanoparticles, it did not sufficiently last over time and almost reached the maximum release limit at 48 h with 40% discharge of the drug. On the contrary, TGX221-loaded PHB nanoparticle showed a sustained release phase, lasting for at least 6 days and releasing about 65% of entrapped TGX221 only at the end of the 6-day term. From the trend of the release curve, it is reasonable to expect that the release of TGX221 could continue for longer time. The in vitro release study of TGX221-loaded PHB nanoparticles was also performed with 2 ml resuspension immerged in 50 ml H_2O and the release profile was almost the same as that showed in Fig. 2 (data not shown). These results thus indicate that the PHA nanoparticles could efficiently and effectively extend the release of TGX221 and could be eventually used for controlled delivery of the drug.

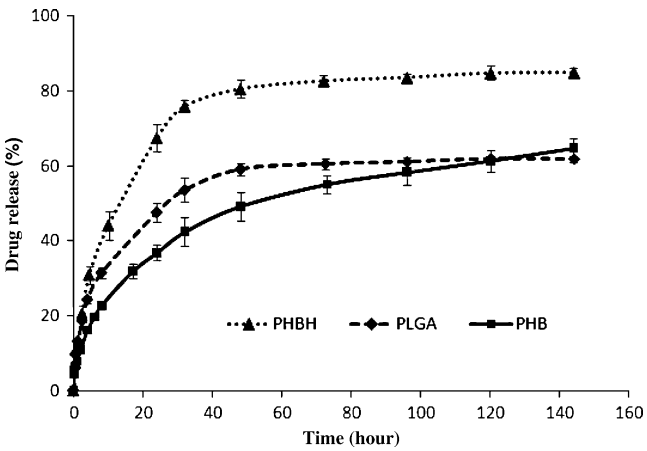

Fig. 2 In vitro release profiles of TGX221-loaded PHB, PHBHHx, and PLGA nanoparticles

In vitro cytotoxicity evaluation of PHA and PLGA nanoparticles

The cytotoxic effect of PHA and PLGA nanoparticles was evaluated in vitro using the NIH/3T3 fibroblast cell line in a crystal violet staining-based colorimetric assay. Figure 3 shows proliferation of NIH/3T3 fibroblast cells incubated with different nanoparticles at doses of 0.1 g/l, 0.05 g/l, and 0.01 g/l, respectively, as a percentage of the untreated control. All PHA-based nanoparticles showed excellent biocompatibility at concentrations between 0.01 and 0.1 g/l. However, in agreement with the previous reports (Muller et al. 1996), decreased cell proliferation was observed in the group treated with PLGA nanoparticles. On the contrary, PHA nanoparticles could promote cell growth especially at low concentration. PHA copolymers with medium-chain-length component such as PHBHHx showed the highest bioactivity in terms of proliferation stimulation. These findings show that, at certain concentration, PHA-based nanoparticles promote cell proliferation, thus narrowing the window of their use in cancer treatment.

In vitro inhibition of cancer cell lines by TGX221-loaded PHA nanoparticle

Because of their features in drug release and their bioactivity profile, TGX221-loaded PHB nanoparticles were used for testing growth inhibition of cancer cell lines. The in vitro cytotoxic activity of TGX221-loaded PHB nanoparticles, drug-free nanoparticles, and free TGX221 were evaluated by the crystal violet staining-based colorimetric assay using the PC3, BT-474, and HCT-116 cell lines, respectively. As shown in Fig. 4, the relative growth of PC3 cell line was evaluated after incubation for 72 h with either TGX221-loaded PHB nanoparticles or drug-free nanoparticles or free TGX221. Both TGX221-loaded PHB nanoparticles and free TGX221 could inhibit the growth of PC3 cell line when medium was changed every 24 h. Of note, these two experimental groups showed matching responses to the treatment: only 10–15% of decrease was observed when either 20 μM of TGX221 or an equal amount of drug-loaded nanoparticle was used (Fig. 4b). On the other hand, likely because of TGX221 instability in cells, when only half of the medium was changed at 32 h, the difference between the free TGX221-treated group and the drug-loaded nanoparticles-treated group was more evident. Exposure to TGX221-loaded nanoparticles reduced cell growth by 15% at doses as low as 0.2 μM. Moreover, cells treated with 20 μM TGX221-loaded nanoparticles proliferated 45% less than the untreated group (Fig. 4a, c). The long-term effect of drug-loaded nanoparticles was likely due to the sustained release of TGX221 which continuously inhibited cell growth. Consistently, western blot analysis of phosphorylated PKB/Akt, a downstream target of PI3K, revealed that administration of TGX221-loaded nanoparticles led to a significant inhibition of the PI3K pathway (Fig. 5). At 2 h after treatment with drug-loaded PHB nanoparticles or free TGX221 (0.2, 2, and 20 μM), PC3 cells showed a significant reduction of the activity of the p110β PI3K isoform, as evidenced by the decreased LPA-mediated triggering of Akt/PKB phosphorylation (Fig. 5). However, PHB nanoparticles with equal amounts of entrapped drug showed p110β inhibition only at 2 and 20 μM. The reduced efficacy of lower doses of nanoparticles was likely due to the fact that only about 10% of entrapped TGX221 was released from the nanoparticle at the end of 2 h, thus reaching levels too low to impact on p110β activity. Nonetheless, the effect appeared selective for p110β as only at doses reaching 20 μM TGX221 were found to inhibit the p110α isoform.

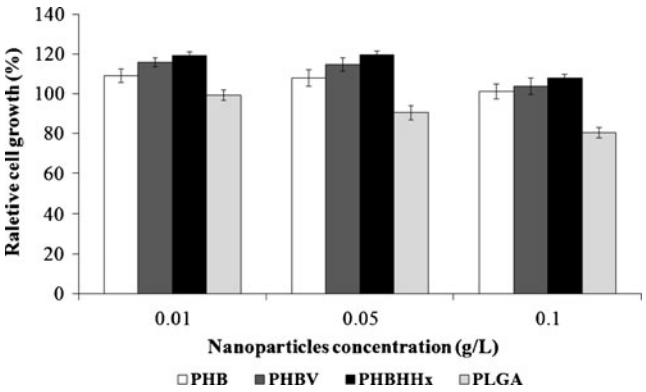

Fig. 3 Cytotoxicity evaluation of PHA and PLGA nanoparticles. NIH/3T3 fibroblast cell line was cultured with different type of nanoparticles. Cells were seeded in 96-well plates and incubated with different concentrations (0.01–0.1 g/l) of the nanoparticles in DMEM for 48 h. Cell number was qualified by crystal violet staining-based colorimetric assay. The cell number of untreated control group was considered as 100%. *$P<0.05$, based on repeated measures ANOVA (Student's t test). Data shown as mean±SD ($n=3$) with three plates in each experiment of the specific absorbance

The inhibitory effect of TGX221-loaded PHBHHx nanoparticles on cell growth was also tested, and results showed that empty PHBHHx particles promote growth of PC3 cells (Fig. 4d). In agreement, the growth inhibition of 20 μM TGX-loaded PHBHHx nanoparticles was lower than that of 20 μM TGX-loaded PHB nanoparticles. The observation that nanoparticles other than PHB promote proliferation and counteract TGX221 activity indicates that PHB is the most promising carrier for anti-cancer treatments.

As expected, treatment with TGX221 was more effective in the PTEN-deficient/p110β-dependent PC3 cells than in HCT-116 and BT-474 cells, carrying K-Ras or PIK3CA mutations, respectively (Fig. 6a). Only 20 μM TGX221-loaded PHB nanoparticles could weakly inhibit cell growth

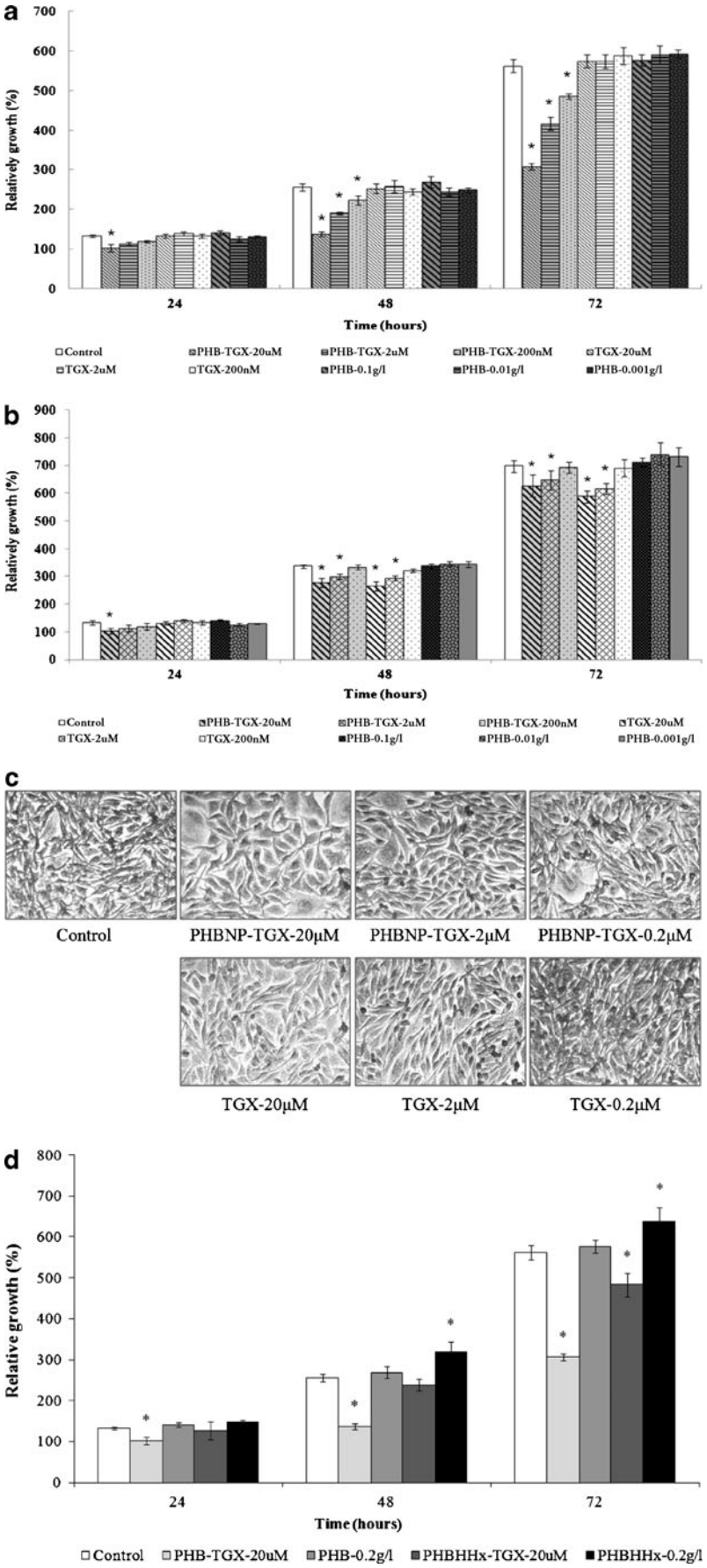

Fig. 4 Growth inhibitions of PC3 cell line treated with TGX221-loaded PHB nanoparticles, drug-free nanoparticles, and free TGX221. Cells were seeded in 96-well plates and incubated with different concentrations (0.2–20 μM) of free TGX221 or drug-loaded PHB nanoparticles in DMEM medium for 72 h. Cell number was qualified by crystal violet staining-based colorimetric assay. The cell number of untreated control group was considered as 100%. *$P<0.05$, based on repeated measures ANOVA (Student's t test). Data shown as mean±SD ($n=3$) with three plates in each experiment of the specific absorbance. **a** Two hundred microliters of DMEM medium was added in each well and half of the medium was removed and supplemented with fresh medium at 32 h. **b** One hundred microliters of DMEM was added in each well and medium was changed every 24 h. **c** Crystal violet staining of PC3 cell line treated with TGX221-loaded PHB nanoparticles or free TGX221. The culture method was the same as that of (**b**). **d** Growth inhibition effect comparison of 20 μM TGX221-loaded PHB/PHBHHx nanoparticles. Two hundred microliters of DMEM medium was added in each well and half of the medium was removed and supplemented with fresh medium at 32 h

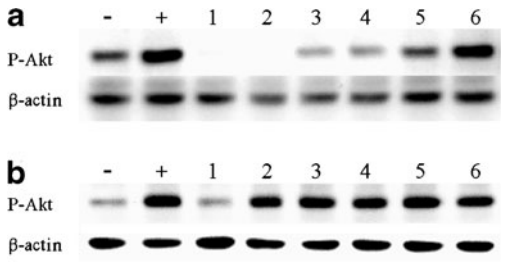

Fig. 5 Analysis of Akt phosphorylation after treated with 0.2, 2, and 20 μM free TGX221 or TGX221-loaded PHB nanoparticle. **a** Cells were stimulated with 10 μM LPA (which could activate p110β isoform) for 5 min. **b** Cells were stimulated with 1 μM insulin (which could activate p110α isoform) for 5 min. − negative control, cells were not treated with any inhibitor and stimulant; + positive control, cells were treated with only stimulant (LPA or insulin). *1* 20 μM TGX221, *2* 2 μM TGX221, *3* 0.2 μM TGX221, *4* 20 μM TGX221-loaded PHB NP, *5* 2 μM TGX221-loaded PHB NP, *6* 0.2 μM TGX221-loaded PHB NP

at 72 h (Fig. 6b). Overall, these results indicate that entrapment of TGX221 in PHA nanoparticles does not change the selectivity of TGX221 against p110β and results in a promising delivery strategy.

Discussion

Activation of the PI3K signaling pathway is frequently found in common human cancers (Liu et al. 2009). However, recent studies have indicated that p110α and p110β exert distinct functions in cell signaling and tumorigenesis. Specifically, p110α is essential for the signaling and growth of tumors driven by PIK3CA mutations and/or oncogenic RTKs/Ras, whereas p110β is the major isoform involved in tumorigenesis in conditions of PTEN loss. Several pan-PI3K inhibitors are currently being evaluated in clinical studies but the obvious disadvantage of using pan-PI3K inhibitors are potential side

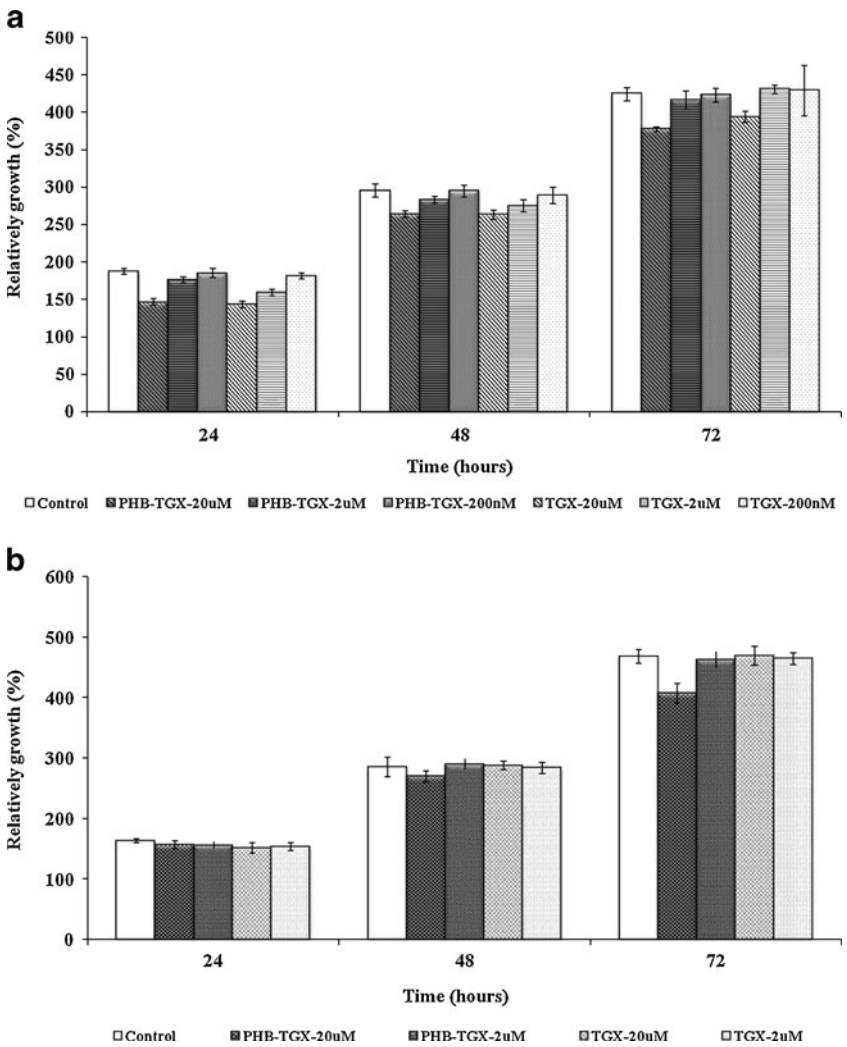

Fig. 6 Growth inhibitions of BT-474 and HCT-116 cell lines treated with TGX221-loaded PHB nanoparticles, drug-free nanoparticles, and free TGX221. Cells were seeded in 96-well plates and incubated with different concentrations (0.2–20 μM) of free TGX221 or drug-loaded PHB nanoparticles in DMEM and McCoy's 5A medium, respectively, for 72 h. Cell number was qualified by crystal violet staining-based colorimetric assay. The cell number of untreated control group was considered as 100%. *$P<0.05$, based on repeated measures ANOVA (Student's t test). Data shown as mean±SD ($n=3$) with three plates in each experiment of the specific absorbance. **a** Growth inhibition of BT-474 cell line. DMEM medium was changed every 24 h. **b** Growth inhibition of HCT-116 cell line. Two hundred microliters of McCoy's 5A medium was added in each well and half of the medium was removed and supplemented with fresh medium at 32 h

effects such as diabetes, sterility, and immune suppression. Nonetheless, different p110 isoforms possess specific functions and inhibitors selective for specific p110 isoforms are expected to show a reduction in those unwanted side effects. For example, genetic blockade of p110β was found to protect from breast cancer but to cause partial insulin resistance (Ciraolo et al. 2008). At present, p110β pharmacological inhibitors have been identified and TGX221 presently represents the molecule with highest selectivity (Chaussade et al. 2007; Jackson et al. 2005). Nonetheless, while TGX221 can be used for in vitro studies, its use in preclinical and clinical studies has been limited by its poor pharmacokinetic properties. This study was thus aimed at finding a formulation of TGX221 that could improve its bioavailability and extend its in vivo half-life. TGX221 was entrapped at 93–97% efficiency in PHA nanoparticles, thus indicating an advantage of PHA as a delivery carrier of hydrophobic drugs. Amounts of TGX221 and PHA nanoparticles had to be precisely balanced because PHA particles are known to promote cell proliferation at low concentration, and this might represent a potential drawback when blocking cancer cell growth is the goal. This is in agreement with previous reports showing that PHBVHHx nanoparticles could increase proliferation by stimulating a rapid increase of cytosolic calcium influx in HaCaT cells (Ji et al. 2008). Several studies also indicated that cell proliferation can be stimulated by 3-hydroxybutyrate (HB), the main component and degradation product of PHB, PHBV, and PHBHHx (Cheng et al. 2005, 2006). However, the concentration of nanoparticles used in our study was calculated to avoid significant effects on cell proliferation. Furthermore, maximal inhibition of proliferation was achieved by a concentration of TGX221 of 20 μM where the corresponding amount of PHB nanoparticles was about 0.1 g/l, a concentration much higher than that of 0.01–0.05 g/l reported to promote cell proliferation (Ji et al. 2008).

In this study, three different cancer cell lines (PC3, BT-474, and HCT-116) with different genetic background were tested to evaluate the potential cytotoxic effects of TGX221-loaded PHA nanoparticles. Interestingly, efficacy in proliferation arrest was significant in PC3 cells, while in the other two lines only 5% to 10% growth inhibition could be observed. Interestingly, this is in line with the current view of p110β involvement in cancer where p110β is critically supporting proliferation when cells lose expression of the phosphatase PTEN (Wee et al. 2008). Consistently, while prostate cancer cells PC3 cells are PTEN deficient, BT-474 breast cancer and HCT-116 colon cancer cells express a wild-type PTEN. In further agreement, low dosage of TGX221-loaded nanoparticles had little effect on HCT-116 colon cancer cells where growth mainly depended on a hotspot mutation in PIK3CA gene and on the expression of a hyperactive p110α isoform. Only the 20 μM TGX221-loaded nanoparticle group showed about 13% inhibition at 72 h. This can explained by the fact that TGX221 can also inhibit p110α isoform at high concentrations and shows an IC_{50} of 5 μM against p110α in assays with purified enzymes. Although in vivo this IC_{50} might be higher, our use of TGX221 at 20 μM resided well beyond its selectivity limit.

Further studies are needed to evaluate the efficacy of TGX221-loaded PHA nanoparticles in vivo. Indeed, the behavior of these nanoparticles in experimental animal models shows that this is potentially an interesting route to follow. Of note, one of the advantages of PHA nanoparticles is the possibility of modification of their surface to achieve tissue-specific drug delivery in vivo. To this aim, the PhaP nanoparticle protein can be fused to other proteins of therapeutic interest: for example, PhaP fusion proteins exposing tissue-specific markers such as human αα1-acid glycoprotein (hAGP) or human epidermal growth factor (hEGF) target macrophages or EGF-responding cancer cells, respectively (Yao et al. 2008). In these conditions, while control nanoparticles concentrate in the liver, the modified PHA biopolymers accumulate in targeted cells. Thus, it would be of interest to investigate the ligand–PhaP–PHA nanoparticle-specific drug delivery system combined with anti-cancer drugs such as PI3K inhibitors. This technique might in principle open the way to an improvement in drug delivery targeting cancer cells but leaving out healthy cells, thus reducing unwanted side effects.

Overall, this study represents to our knowledge the first report concerning the application of PHA as a drug delivery carrier in anti-cancer study. Our result indicated the entrapment of TGX221 into PHA nanoparticles could sufficiently extend its half-life and thus enhance its bioavailability. While in vivo anti-cancer evaluation of the TGX221-loaded PHA nanoparticles in animal models is still needed, the proven effectiveness in cell-based assays of this technique opens the way to similar formulation of other PI3K inhibitors. Because poor bioavailability and limited in vivo half-life are rather common features of PI3K inhibitors that usually are highly hydrophobic compounds, this PHA nanoparticle-based drug delivery system might have further applications in the field. Future studies might thus explore the possibility of delivering PI3K inhibitors specifically towards cancer cells, thus enhancing efficacy and further reducing the side effects due to targeting of the protein in healthy tissues.

Acknowledgments This work was supported by grants from the National Natural Science Foundation of China (30801059), the Doctoral Fund of Ministry of Education of China (200806981053), and AIRC, Regione Piemonte, Cariplo.

References

Bader AG, Kang SY, Zhao L, Vogt PK (2005) Oncogenic pi3k deregulates transcription and translation. Nat Rev Cancer 5 (12):921–929. doi:10.1038/nrc1753

Chaussade C, Rewcastle GW, Kendall JD, Denny WA, Cho K, Gronning LM, Chong ML, Anagnostou SH, Jackson SP, Daniele N, Shepherd PR (2007) Evidence for functional redundancy of class ia pi3k isoforms in insulin signalling. Biochem J 404:449–458. doi:10.1042/bj20070003

Cheng S, Wu Q, Yang F, Xu M, Leski M, Chen GQ (2005) Influence of dl-beta-hydroxybutyric acid on cell proliferation and calcium influx. Biomacromolecules 6(2):593–597. doi:10.1021/bm049465y

Cheng S, Chen GQ, Leski M, Zou B, Wang Y, Wu Q (2006) The effect of d, l-beta-hydroxybutyric acid on cell death and proliferation in l929 cells. Biomaterials 27(20):3758–3765. doi:10.1016/j.biomaterials.2006.02.046

Chin L, Meyerson M, Aldape K, Bigner D, Mikkelsen T, VandenBerg S, Kahn A, Penny R, Ferguson ML, Gerhard DS, Getz G, Brennan C, Taylor BS, Winckler W, Park P, Ladanyi M, Hoadley KA, Verhaak RGW, Hayes DN, Spellman PT, Absher D, Weir BA, Ding L, Wheeler D, Lawrence MS, Cibulskis K, Mardis E, Zhang JH, Wilson RK, Donehower L, Wheeler DA, Purdom E, Wallis J, Laird PW, Herman JG, Schuebel KE, Weisenberger DJ, Baylin SB, Schultz N, Yao J, Wiedemeyer R, Weinstein J, Sander C, Gibbs RA, Gray J, Kucherlapati R, Lander ES, Myers RM, Perou CM, McLendon R, Friedman A, Van Meir EG, Brat DJ, Mastrogianakis GM, Olson JJ, Lehman N, Yung WKA, Bogler O, Berger M, Prados M, Muzny D, Morgan M, Scherer S, Sabo A, Nazareth L, Lewis L, Hall O, Zhu YM, Ren YR, Alvi O, Yao JQ, Hawes A, Jhangiani S, Fowler G, San Lucas A, Kovar C, Cree A, Dinh H, Santibanez J, Joshi V, Gonzalez-Garay ML, Miller CA, Milosavljevic A, Sougnez C, Fennell T, Mahan S, Wilkinson J, Ziaugra L, Onofrio R, Bloom T, Nicol R, Ardlie K, Baldwin J, Gabriel S, Fulton RS, McLellan MD, Larson DE, Shi XQ, Abbott R, Fulton L, Chen K, Koboldt DC, Wendl MC, Meyer R, Tang YZ, Lin L, Osborne JR, Dunford-Shore BH, Miner TL, Delehaunty K, Markovic C, Swift G, Courtney W, Pohl C, Abbott S, Hawkins A, Leong S, Haipek C, Schmidt H, Wiechert M, Vickery T, Scott S, Dooling DJ, Chinwalla A, Weinstock GM, O'Kelly M, Robinson J, Alexe G, Beroukhim R, Carter S, Chiang D, Gould J, Gupta S, Korn J, Mermel C, Mesirov J, Monti S, Nguyen H, Parkin M, Reich M, Stransky N, Garraway L, Golub T, Protopopov A, Perna I, Aronson S, Sathiamoorthy N, Ren G, Kim H, Kong SK, Xiao YH, Kohane IS, Seidman J, Cope L, Pan F, Van Den Berg D, Van Neste L, Yi JM, Li JZ, Southwick A, Brady S, Aggarwal A, Chung T, Sherlock G, Brooks JD, Jakkula LR, Lapuk AV, Marr H, Dorton S, Choi YG, Han J, Ray A, Wang V, Durinck S, Robinson M, Wang NJ, Vranizan K, Peng V, Van Name E, Fontenay GV, Ngai J, Conboy JG, Parvin B, Feiler HS, Speed TP, Socci ND, Olshen A, Lash A, Reva B, Antipin Y, Stukalov A, Gross B, Cerami E, Wang WQ, Qin LX, Seshan VE, Villafania L, Cavatore M, Borsu L, Viale A, Gerald W, Topal MD, Qi Y, Balu S, Shi Y, Wu G, Bittner M, Shelton T, Lenkiewicz E, Morris S, Beasley D, Sanders S, Sfeir R, Chen J, Nassau D, Feng L, Hickey E, Schaefer C, Madhavan S, Buetow K, Barker A, Vockley J, Compton C, Vaught J, Fielding P, Collins F, Good P, Guyer M, Ozenberger B, Peterson J, Thomson E, Cancer Genome Atlas Research Network (2008) Comprehensive genomic characterization defines human glioblastoma genes and core pathways. Nature 455(7216):1061–1068. doi:10.1038/nature07385

Ciraolo E, Iezzi M, Marone R, Marengo S, Curcio C, Costa C, Azzolino O, Gonella C, Rubinetto C, Wu HY, Dastru W, Martin EL, Silengo L, Altruda F, Turco E, Lanzetti L, Musiani P, Ruckle T, Rommel C, Backer JM, Forni G, Wymann MP, Hirsch E (2008) Phosphoinositide 3-kinase p110 beta activity: key role in metabolism and mammary gland cancer but not development. Sci Signal 1(36). doi:10.1126/scisignal.1161577

Gursel I, Korkusuz F, Turesin F, Alaeddinoglu NG, Hasirci V (2001) In vivo application of biodegradable controlled antibiotic release systems for the treatment of implant-related osteomyelitis. Biomaterials 22(1):73–80

Jackson SP, Schoenwaelder SM, Goncalves I, Nesbitt WS, Yap CL, Wright CE, Kenche V, Anderson KE, Dopheide SM, Yuan YP, Sturgeon SA, Prabaharan H, Thompson PE, Smith GD, Shepherd PR, Daniele N, Kulkarni S, Abbott B, Saylik D, Jones C, Lu L, Giuliano S, Hughan SC, Angus JA, Robertson AD, Salem HH (2005) Pi 3-kinase p110 beta: a new target for antithrombotic therapy. Nat Med 11(5):507–514. doi:10.1038/nm1232

Jeong I, Kim BS, Lee H, Lee KM, Shim I, Kang SK, Yin CS, Hahm DH (2009) Prolonged analgesic effect of PLGA-encapsulated bee venom on formalin-induced pain in rats. Int J Pharm 380(1–2):62–66. doi:10.1016/j.ijpharm.2009.06.034

Ji Y, Li XT, Chen GQ (2008) Interactions between a poly(3-hydroxybutyrate-co-3-hydroxyvalerate-co-3-hydroxyhexanoate) terpolyester and human keratinocytes. Biomaterials 29(28):3807–3814. doi:10.1016/j.biomaterials.2008.06.008

Keniry M, Parsons R (2008) The role of pten signaling perturbations in cancer and in targeted therapy. Oncogene 27(41):5477–5485. doi:10.1038/onc.2008.248

Koosha F, Muller RH, Davis SS (1989) Polyhydroxybutyrate as a drug carrier. Crit Rev Ther Drug Carr Syst 6(2):117–130

Kueng W, Silber E, Eppenberger U (1989) Quantification of cells cultured on 96-well plates. Anal Biochem 182(1):16–19

Langer R (1998) Drug delivery and targeting. Nature 392(6679):5–10

Leevers SJ, Vanhaesebroeck B, Waterfield MD (1999) Signalling through phosphoinositide 3-kinases: the lipids take centre stage. Curr Opin Cell Biol 11(2):219–225

Li Q, Wang Y, Feng NP, Fan ZZ, Sun J, Nan YL (2008) Novel polymeric nanoparticles containing tanshinone IIa for the treatment of hepatoma. J Drug Target 16(10):725–732. doi:10.1080/10611860802374303

Liu Q, Chen GQ (2008) In vitro biocompatibility and degradation of terpolyester 3hb-co-4hb-co-3hhx, consisting of 3-hydroxybutyrate, 4-hydroxybutyrate and 3-hydroxyhexanoate. J Biomater Sci Polym Ed 19(11):1521–1533

Liu PX, Cheng HL, Roberts TM, Zhao JJ (2009) Targeting the phosphoinositide 3-kinase pathway in cancer. Nat Rev Drug Discov 8(8):627–644. doi:10.1038/nrd2926

Lu XY, Zhang YL, Wang L (2010) Preparation and in vitro drug-release behavior of 5-fluorouracil-loaded poly(hydroxybutyrate-co-hydroxyhexanoate) nanoparticles and microparticles. J Appl Polym Sci 116(5):2944–2950. doi:10.1002/app.31806

Muller RH, Maassen S, Weyhers H, Specht F, Lucks JS (1996) Cytotoxicity of magnetite-loaded polylactide, polylactide/glycolide particles and solid lipid nanoparticles. Int J Pharm 138(1):85–94

Mundargi RC, Babu VR, Rangaswamy V, Patel P, Aminabhavi TM (2008) Nano/micro technologies for delivering macromolecular therapeutics using poly(d, l-lactide-co-glycolide) and its derivatives. J Control Release 125(3):193–209. doi:10.1016/j.jconrel.2007.09.013

Parsons DW, Jones S, Zhang XS, Lin JCH, Leary RJ, Angenendt P, Mankoo P, Carter H, Siu IM, Gallia GL, Olivi A, McLendon R, Rasheed BA, Keir S, Nikolskaya T, Nikolsky Y, Busam DA, Tekleab H, Diaz LA, Hartigan J, Smith DR, Strausberg RL, Marie SKN, Shinjo SMO, Yan H, Riggins GJ, Bigner DD, Karchin R, Papadopoulos N, Parmigiani G, Vogelstein B, Velculescu VE, Kinzler KW (2008) An integrated genomic analysis of human glioblastoma multiforme. Science 321 (5897):1807–1812. doi:10.1126/science.1164382

Perez C, Sanchez A, Putnam D, Ting D, Langer R, Alonso MJ (2001) Poly(lactic acid)-poly(ethylene glycol) nanoparticles as new carriers for the delivery of plasmid DNA. J Control Release 75 (1–2):211–224

Rossi S, Azghani AO, Omri A (2004) Antimicrobial efficacy of a new antibiotic-loaded poly(hydroxybutyric-co-hydroxyvaleric acid) controlled release system. J Antimicrob Chemother 54(6):1013–1018. doi:10.1093/jac/dkh477

Saad B, Ciardelli G, Matter S, Welti M, Uhlschmid GK, Neuenschwander P, Suter UW (1996a) Cell response of cultured macrophages, fibroblasts, and co-cultures of Kupffer cells and hepatocytes to particles of short-chain poly (r)-3-hydroxybutyric acid. J Mater Sci Mater Med 7(1):56–61

Saad B, Ciardelli G, Matter S, Welti M, Uhlschmid GK, Neuenschwander P, Suter UW (1996b) Characterization of the cell response of cultured macrophages and fibroblasts to particles of short-chain poly (r)-3-hydroxybutyric acid. J Biomed Mater Res 30(4):429–439

Shi JJ, Votruba AR, Farokhzad OC, Langer R (2010) Nanotechnology in drug delivery and tissue engineering: from discovery to applications. Nano Lett 10(9):3223–3230. doi:10.1021/nl102184c

Steinbuchel A (2001) Perspectives for biotechnological production and utilization of biopolymers: metabolic engineering of polyhydroxyalkanoate biosynthesis pathways as a successful example. Macromol Biosci 1(1):1–24

Sun J, Dai ZW, Zhao Y, Chen GQ (2007) In vitro effect of oligohydroxyalkanoates on the growth of mouse fibroblast cell line l929. Biomaterials 28(27):3896–3903. doi:10.1016/j.biomaterials.2007.05.011

Thomas RK, Baker AC, DeBiasi RM, Winckler W, LaFramboise T, Lin WM, Wang M, Feng W, Zander T, MacConnaill LE, Lee JC, Nicoletti R, Hatton C, Goyette M, Girard L, Majmudar K, Ziaugra L, Wong KK, Gabriel S, Beroukhim R, Peyton M, Barretina J, Dutt A, Emery C, Greulich H, Shah K, Sasaki H, Gazdar A, Minna J, Armstrong SA, Mellinghoff IK, Hodi FS, Dranoff G, Mischel PS, Cloughesy TF, Nelson SF, Liau LM, Mertz K, Rubin MA, Moch H, Loda M, Catalona W, Fletcher J, Signoretti S, Kaye F, Anderson KC, Demetri GD, Dummer R, Wagner S, Herlyn M, Sellers WR, Meyerson M, Garraway LA (2007) High-throughput oncogene mutation profiling in human cancer. Nat Genet 39:347–351. doi:10.1038/ng1975

Vanhaesebroeck B, Leevers SJ, Panayotou G, Waterfield MD (1997) Phosphoinositide 3-kinases: a conserved family of signal transducers. Trends Biochem Sci 22(7):267–272

Wang ZX, Itoh Y, Hosaka Y, Kobayashi I, Nakano Y, Maeda I, Umeda F, Yamakawa J, Kawase M, Yagi K (2003) Novel transdermal drug delivery system with polyhydroxyalkanoate and starburst polyamidoamine dendrimer. J Biosci Bioeng 95(5):541–543

Wee S, Wiederschain D, Maira SM, Loo A, Miller C, DeBeaumont R, Stegmeier F, Yao YM, Lengauer C (2008) PTEN-deficient cancers depend on PIK3CB. Proc Natl Acad Sci USA 105 (35):13057–13062. doi:10.1073/pnas.0802655105

Wu Q, Wang Y, Chen GQ (2009) Medical application of microbial biopolyesters polyhydroxyalkanoates. Artif Cells Blood Substit Immobil Biotechnol 37(1):1–12. doi:10.1080/10731190802664429

Xiao XQ, Zhao Y, Chen GQ (2007) The effect of 3-hydroxybutyrate and its derivatives on the growth of glial cells. Biomaterials 28 (25):3608–3616. doi:10.1016/j.biomaterials.2007.04.046

Xiong YC, Yao YC, Zhan XY, Chen GQ (2010) Application of polyhydroxyalkanoates nanoparticles as intracellular sustained drug-release vectors. J Biomater Sci Polym Ed 21(1):127–140. doi:10.1163/156856209x410283

Yao YC, Zhan XY, Zhang J, Zou XH, Wang ZH, Xiong YC, Chen J, Chen GQ (2008) A specific drug targeting system based on polyhydroxyalkanoate granule binding protein phap fused with targeted cell ligands. Biomaterials 29(36):4823–4830. doi:10.1016/j.biomaterials.2008.09.008